

## Cation effect on gel – sol transition of kappa carrageenan

Önder Pekcan<sup>1</sup> (✉) and Özlem Tari<sup>2</sup>

<sup>1</sup> Işık University, Department of Physics, Kumbaba, Şile, 34980 Istanbul, Turkey

<sup>2</sup> Istanbul Technical University, Department of Physics, Maslak, 34469 Istanbul, Turkey

E-mail: pekcan@isikun.edu.tr; Fax: +90 216 7121474

Received: 10 October 2007 / Accepted: 21 November 2007

Published online: 11 December 2007 – © Springer-Verlag 2007

### Summary

The steady state fluorescence (SSF) technique was employed to study gel - sol transitions of kappa carrageenan in *NaCl*, *KCl* and *CaCl<sub>2</sub>* solutions. Pyranine was used as a fluorescence probe for monitoring these transitions. Scattered light,  $I_{sc}$  and fluorescence intensity,  $I$  was monitored against temperature to determine the gel - sol ( $T_{gs}$ ) transition temperatures and exponents. It was observed that  $T_{gs}$  values are strongly correlated to the *NaCl*, *KCl* and *CaCl<sub>2</sub>* contents. The weight average degree of polymerization,  $DP_w$  and gel fraction  $G$ , exponents ( $\gamma$  and  $\beta$ ) were measured and found to be in accord with the classical Flory – Stockmayer Model.

### Introduction

The gels obtained from polymers of biological origin are an important category because they have the advantage of utilizing water as the solvent and thus have many applications in the food industry. These are physical gels since the gelation process is reversible. Two types of biopolymer gels are particularly important; protein gels and polysaccharide gels. Polysaccharides are natural polymers found in plants, algae, animals and bacteria; some are electrically neutral, while others are charged. Agarose and amylose are neutral polysaccharides whereas carrageenans are electrically charged polysaccharides that form thermoreversible gels [1].

Carrageenan is the name of a family of sulphated galactans extracted from marine red algae. Different types of carrageenan may be distinguished by their primary structure.  $\kappa$ -carrageenan is composed of alternating disaccharide of  $\alpha$  (1 $\rightarrow$ 3)-D-galactose and  $\beta$  (1 $\rightarrow$ 4)-3,6-anhydro-D-galactose and contains one sulphate group per disaccharide unit at carbon 2 of the 1,3 linked galactose unit [2]. Carrageenan is one of the most important polysaccharides with a wide range of food applications. They are versatile as food additives, being capable of binding water, promoting gel formation, and acting as thickeners and stabilizing agents [3].

It is known that the gelation of kappa carrageenan involves two separate and successive steps; coil-to-helix transition upon cooling and subsequent cation-dependent aggregation between helices [4]. The effect of various cations on the conformational transition of kappa carrageenan has been studied [5, 6]. Rochas and Rinaudo found that the investigated cations may be divided into three categories

with respect to their helix-promoting efficiency in the case of kappa-carrageenan; non-specific monovalent cations (*Li*, *Na*) < divalent cations (*Ca*, *Mg*) < specific monovalent cations (*K*, *Cs*).

Salt and ion effects on the rheology of  $\kappa$ -carrageenan and phase transition temperatures have been studied by several groups [2, 7 – 12]. The effectiveness of increasing sol-gel and gel-sol temperatures at various salt concentrations were examined by following the sequence of  $K^+ > Ca^{2+} > Na^+$  in *KCl*, *CaCl*<sub>2</sub> and *NaCl* solutions, respectively. The addition of salts such as *NaCl*, *KCl* and *CaCl*<sub>2</sub> at an adequate concentration appears to improve gel strength or elastic modulus of  $\kappa$ -carrageenan gels through enhancing conformational ordering and subsequent aggregation.

The effects of cations and mixtures of cations on kappa carrageenan gelation was studied by electron microscopy and viscoelastic measurements [3, 13]. Organization and association of  $\kappa$ -carrageenan helices under various salt conditions were studied and it is observed that it is possible to tune the various levels of association of  $\kappa$ -carrageenan helices by using mixed salts [14]. Differential scanning calorimetry and extension tests were carried out on kappa carrageenan gels in the presence of the alkali metal salts *LiCl*, *NaCl*, *KCl* and *CsCl* [15]. The microviscosity of the hydrophobic microdomains, the dynamic rheology and molecular conformation was studied in  $\kappa$ -carrageenan systems by means of fluorescence intermolecular excimer forming probe, by dynamic viscometry and by optical rotation, respectively [16].

In this study, gel - sol transitions of  $\kappa$ -carrageenan in *NaCl*, *KCl* and *CaCl*<sub>2</sub> solutions were studied using the steady state fluorescence (SSF) technique. Pyranine (P) was used as fluorescence probe. Using this technique, it is possible to study different microenvironments in which the probe molecules finds itself, including experiments on polymerization [17], chemical gel formation [18, 19], swelling, slow release of the probe molecules from gel [20], metal ion detection [21], affinity of the gels to the target probe molecule like pyranine [22], and examination of the collapsed state phases and volume phase transition of the polymeric gels [23]. It was observed that during gel – sol transition of carrageenan molecules, pyranine intensity *I*, presented a continuous decrease. Scattered light intensity, *I*<sub>sc</sub> was also monitored to detect the changes of turbidity during gel – sol phase transition. The necessary correction on the pyranine intensity was made to produce the real gel – sol transition curves. Gel – sol transition temperatures, *T*<sub>gs</sub> were determined for each curve of samples in various *NaCl*, *KCl* and *CaCl*<sub>2</sub> solutions. It was observed that *T*<sub>gs</sub> values increased by increasing *NaCl*, *KCl* and *CaCl*<sub>2</sub> content. The measured weight average degree of polymerization exponents,  $\gamma$  and gel fraction exponents,  $\beta$ , was found to be in accord with the classical Flory – Stockmayer model during the gel – sol transition.

### Theoretical Considerations

For the critical exponents ( $\gamma$  and  $\beta$ ) near the sol – gel phase transition, classical theories like those of Flory – Stockmayer predict one set of exponents, whereas scaling theories based on lattice percolation predict different exponents. The exponents  $\gamma$  and  $\beta$  for the weight average degree of polymerization, *DP*<sub>w</sub>, and the gel fraction *G* both are equal to unity, independent of the dimensionality in the Flory – Stockmayer model. The critical behavior of the gel fraction *G* and the weight average degree of polymerization, *DP*<sub>w</sub> near the gel point are defined as

$$DP_w \propto (p_c - p)^{-\gamma}, \quad p \rightarrow p_c^- \quad (1)$$

$$G \propto (p - p_c)^\beta, \quad p \rightarrow p_c^+ \quad (2)$$

where the Flory – Stockmayer theory gives  $\beta=1$  and  $\gamma=1$ , independent of the dimensionality, while the percolation studies (using series expansions or computer simulations) give  $\gamma$  and  $\beta$  around 1.80 and 0.41 in three dimension [24, 25].

Flory-Stockmayer theory based on tree approximation, which is also called classical theory or kinetic theory [26, 27]. In this theory the closed loops were ignored. An alternative to this model is the lattice percolation model where monomers are thought to occupy the sites of a periodic lattice [24, 25]. A bond between these lattice sites is formed randomly with probability  $p$ . At a certain bond concentration  $p_c$ , defined as the percolation threshold, the infinite cluster is formed in the thermodynamic limit. This is called the gel in polymer language. The polymeric system is in the sol state below the critical conversion,  $p_c$ .

Experimental techniques used for monitoring the gel to sol transition should be very sensitive to the structural changes, and should not disturb the system mechanically. Fluorescence technique is of particularly useful for studying of detailed structural aspects of the gels. The fluorescence technique is based on the interpretation of the change in anisotropy, emission and / or excitation spectra, emission intensity, and viewing the lifetimes of embedded dye molecules to monitor the change in their microenvironment [28, 29]. It can be used in two ways for the studies on polymerization and gelation. First, one can add a fluorescence dye as a free probe to the system. By using fluorescence probe it is possible to determine the microenvironment (polarity, viscosity etc.) with in the gel. In the second approach, the fluorescence dye is covalently attached to the polymer, and serves as a polymer – bond label.

In this study, it can be argued that the total fluorescence intensity from the pyranines monitors the average degree of polymerization and the growing gel fraction, for below and above the gel point, respectively. This proportionality can easily be shown by using a Stauffer type argument as follow [24] under the assumption that the monomers are from the sites of a periodic lattice. A cluster is a group of neighbouring occupied sites containing no empty site in between. A single empty site would split the group into two different clusters. For clusters containing  $s$  sites, we define  $n_s$  as the number of such  $s$ -clusters per lattice site. The probability that a site belongs to a cluster of size  $s$  is given by  $n_s s$ . The probability of each lattice site being occupied is  $p$ . There is a probability  $n_s s$  that an arbitrary belongs to an  $s$ -cluster and a probability  $\sum_s n_s s$  that

it belongs to any finite cluster. Thus  $w_s = \frac{n_s s}{\sum_s n_s s}$  is the probability that the cluster to

which an arbitrary occupied site belongs contains exactly  $s$  sites. The average cluster size  $S$  can be calculated by following relation.

$$S = \sum_s w_s s = \frac{\sum_s n_s s^2}{\sum_s n_s s} \quad (3)$$

The definition of the average cluster size is the same for all dimensions, although  $n$  can not be calculated exactly in higher dimensions. This definition is also holds for the bond percolation.

Now, to show that below  $p_c$ , pyranine intensity is proportional to  $S$ , let  $N_p$  be the number of pyranine molecules and  $N_m$  the other molecules in the lattice. Thus, the total lattice site,  $N$  is equal to  $N_p + N_m$ . The probability,  $p_p$ , that an arbitrary site is a pyranine molecule is  $N_p / N$ . The probability,  $P_y$ , that an arbitrary site both is a pyranine and belongs to the  $s$ -cluster can be calculated as a product of  $w_s$  and  $p_p$  as follow

$$P_y = p_p w_s = \frac{p_p n_s s}{\sum n_s s} \quad (4)$$

Thus the total number of pyranine molecules in the clusters including  $s$  sites will be  $P_y s$ . The total fluorescence intensity,  $I$ , which is proportional to the total number of pyranines trapped in the finite clusters, can be calculated as a summation over all  $s$ -clusters

$$I \approx \sum_s P_y s = \sum_s \frac{p_p n_s s}{\sum n_s s} s = \frac{\sum p_p n_s s^2}{\sum n_s s} \quad (5)$$

where  $p_p$  can be taken out of the summation since the concentration of the pyranine is fixed for our work,

$$I \approx p_p \frac{\sum n_s s^2}{\sum n_s s} = p_p S \quad (6)$$

Thus, the last expression shows that the total normalized fluorescent intensity is proportional to the average cluster size. Note that the proportionality factor,  $p_p$  is simply the concentration of the pyranine molecules in the sample cell (or the number of pyranines in the lattice). Intensity will be linearly proportional to the average cluster size, provided that the pyranine concentration is not so high to quench the fluorescence intensity by reabsorption mechanism and no other parameter like viscosity influencing the fluorescence intensity in addition to the concentration of pyranine.

## Materials and Methods

Carrageenan (Sigma) and pyranine were used to prepare gels by dissolving them in distilled hot water (pH 6.5) with  $KCl$ ,  $NaCl$  and  $CaCl_2$  solution at the desired concentration. The pyranine concentration were kept at  $4 \times 10^{-4} M$  low enough to ensure that excitation transfer effects are negligible. The heated carrageenan sol was held at  $80^\circ C$  and was continuously stirred by magnetic stirrer. Then the sol was allowed to cool to room temperature. Mainly three different set of experiments were carried out: The first set samples were prepared with constant carrageenan content (2%) in various  $KCl$  content solutions. These samples were named as C2K0, C2K2, C2K4 and C2K8. The second set samples were prepared with constant carrageenan content (2%) in various  $NaCl$  content solutions. These samples were named as C2Na4, C2Na6, C2Na8 and C2Na1. The last set of samples was prepared in various  $CaCl_2$  content solutions. These samples were named as C2Ca4, C2Ca8 and C2Ca1. The compositions and the symbols of the studied gels with various  $NaCl$ ,  $KCl$  and  $CaCl_2$  solutions are listed in Table 1.

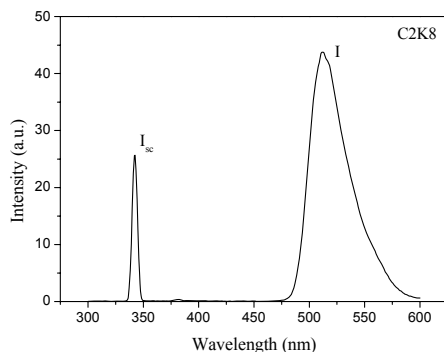


**Figure 1.** Fluorescence spectra of pyranine from C2K8 sample.  $I_{sc}$  and  $I$  present the scattered and emission intensities respectively.

**Table 1.** The compositions, the symbols and the gel - sol ( $T_{gs}$ ) transition temperatures of the studied gels in various  $KCl$ ,  $CaCl_2$  and  $NaCl$  solutions.

Salt content (wt%)	%KCl		%CaCl <sub>2</sub>		%NaCl	
	Gels	$T_{gs}$ (°C)	Gels	$T_{gs}$ (°C)	Gels	$T_{gs}$ (°C)
0	C2K0	55.6	C2Ca0	55.6	C2Na0	55.6
0.2	C2K2	60.7				
0.4	C2K4	65.9	C2Ca4	64.5	C2Na4	54.5
0.6					C2Na6	58.5
0.8	C2K8	76.2	C2Ca8	67.6	C2Na8	59.0
1			C2Ca1	71.7	C2Na1	62.3

The fluorescence intensity measurements were carried out using the Model LS-50 spectrometer of Perkin&Elmer, equipped with temperature controller. A thermocouple immersed in the sample was used to measure the temperature. All measurements were made at front face position and slit widths were kept at 5nm.  $P$  was excited at 360nm during *in situ* experiments and variation in the scattered fluorescence emission intensity of the pyranine was monitored as a function of temperature. Typical fluorescence spectra are presented in Figure 1 where  $I_{sc}$  and  $I$  are shown. Gel – sol transitions were performed in glass tubes of 8mm internal diameter equipped with a heat reservoir. Temperature was monitored and *in situ*, SSF measurements were performed simultaneously using Perkin Elmer spectrometer. The carrageenan sol at 80°C was transferred into the glass cell and left to be cool to room temperature. Both scattered  $I_{sc}$  and fluorescence intensities,  $I$ , were monitored against temperature by using the time drive mode of the spectrometer during gel - sol transitions.

## Results and Discussion

Temperature variation of fluorescence intensities,  $I$  and the scattered light intensities  $I_{sc}$  for the C2K2 and C2Na4 gels during gel sol transition are shown in Figures 2 and 3 respectively.

It is seen in Figures 2 and 3 that,  $I_{sc}$  decreased upon heating the carrageenan samples in both cases indicating that the turbidity of the gels decreased considerably. In the solid phase, carrageenan molecules are in the form of double helix aggregates. During

heating, initially the double helix aggregates are destroyed, and then the double helices are decomposed, which results in the destruction of the gel structure. A representation of the above process is shown in Figure 4. In order to elaborate the above results;  $I$  intensity has to be corrected dividing it by transmitted intensity,  $I_{tr}$  ( $=1 / I_{sc}$ ), because the shape of the excitation light has the character of  $I_{tr}$ . Figure 5 presents the corrected fluorescence intensities,  $I_c$  for C2K2 and C2Na4 samples respectively.

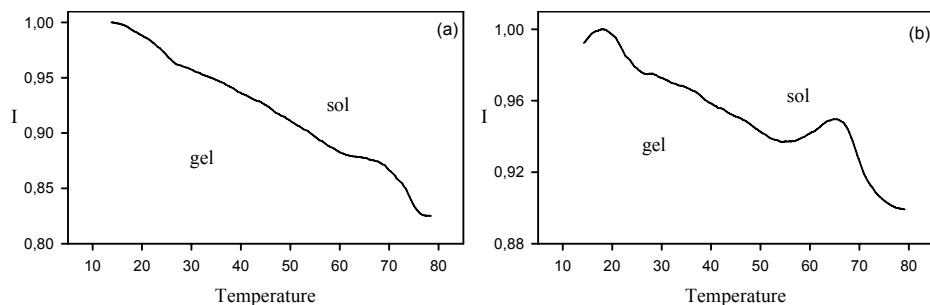


**Figure 2.** Temperature variation of fluorescence intensities for a) C2K2 and b) C2Na4 samples.

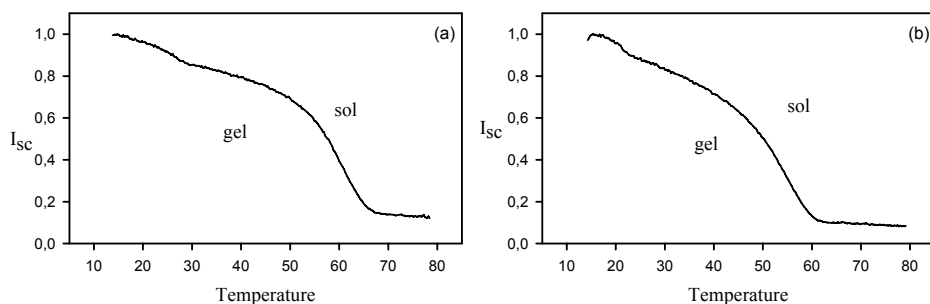


**Figure 3.** Temperature variation of scattered intensities for a) C2K2 and b) C2Na4 samples.

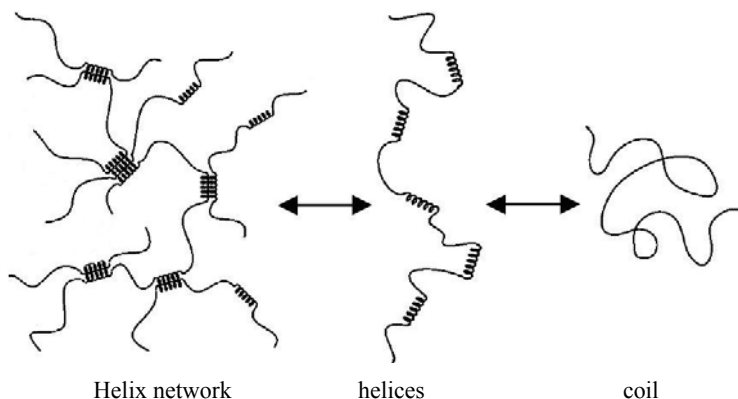


**Figure 4.** Cartoon presentation of gel – sol phase transition and the structure of the helix network (Cayley tree).

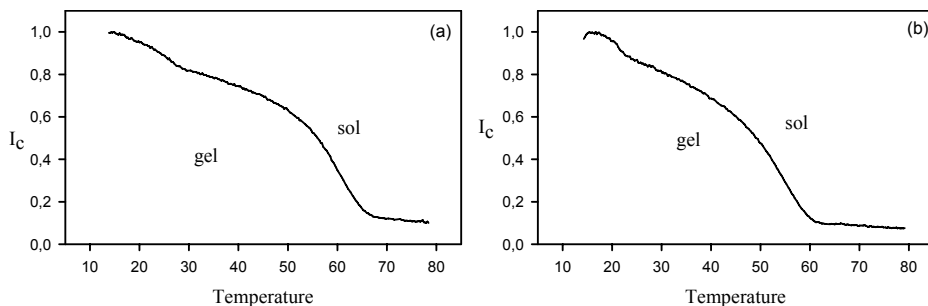


**Figure 5.** Temperature variation of corrected fluorescence intensities for a) C2K2 and b) C2Na4 samples.

The gel sol transition temperatures,  $T_{gs}$  were determined from the position of the extrema of the first derivative of the  $I_c$  curves which are shown in Figures 6a, 6b and 6c and are listed in Table 1 for C2Na4, C2Na6 and C2Na1 samples respectively. In Figure 7, the variation of  $T_{gs}$  versus  $KCl$ ,  $NaCl$  and  $CaCl_2$  content for a given carrageenan concentration (2%) are presented respectively. For high carrageenan content samples, gel - sol transitions required higher temperatures as expected.

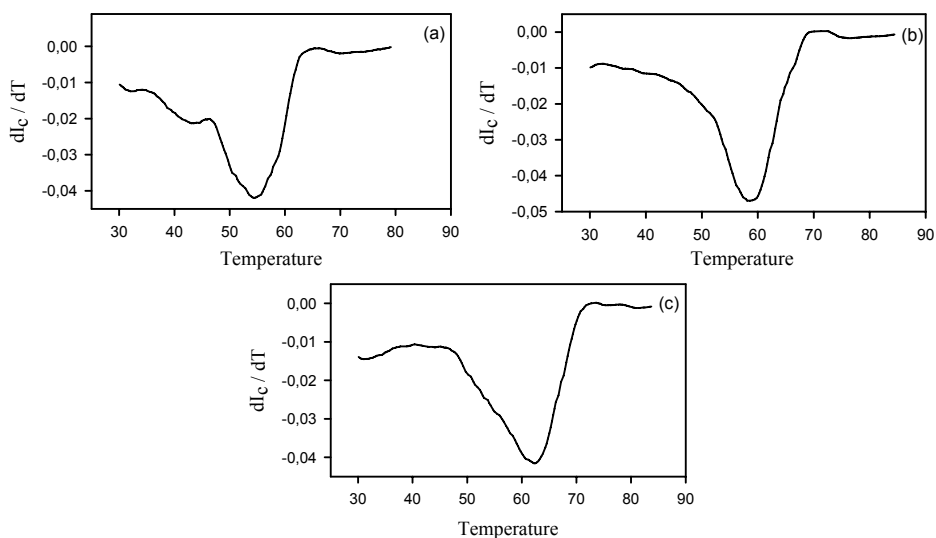


**Figure 6.** The first derivative of  $I_c$  curves,  $dI_c/dT$  versus temperature,  $T$  for a) C2Na4, b) C2Na6, c) C2Na1 samples. The peak positions of  $dI_c/dT$  curves produce  $T_{gs}$  temperatures.

Gelation theory often makes the assumption that the conversion factor  $p$  determines the behavior of the gelation process, in the mean time  $p$  may depend on temperature [30]. Therefore above the gel point i.e. for  $T > T_{gs}$  the fluorescence intensity,  $I_c$  measures the weight average degree of polymerization (or average cluster size) in the gel - sol transition path. However for  $T < T_{gs}$  the intensity,  $I_c$  measures the gel fraction  $G$ , the fraction of the monomers that belong to the macroscopic network. Then the Eqs. (1) and (2) can be written in the following form

$$I_c \propto DP_w \propto (T - T_{gs})^{-\gamma}, \quad T \rightarrow T_{gs}^+ \tag{7}$$

$$I_{cc} = (I_c - I_{ms}) \propto G \propto (T_{gs} - T)^\beta, \quad T \rightarrow T_{gs}^- \tag{8}$$

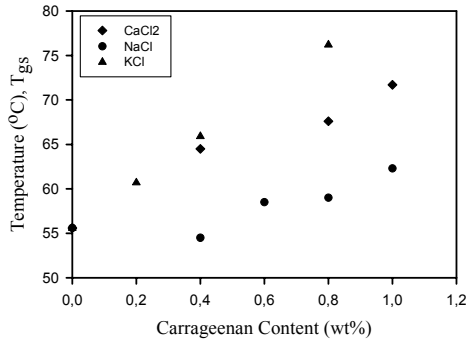


**Figure 7.** The behavior of transition temperature,  $T_{gs}$  versus carrageenan content in  $NaCl$ ,  $KCl$  and  $CaCl_2$  solutions.

Here  $I_{cc}$  solely present the pyranines embedded in the growing gel fraction,  $G$  i.e.  $I_{cc}$  is produced by subtracting the mirror symmetry of  $I_c$  intensity belong to pyranines embedded in the small clusters from the total  $I_c$  intensity. Figures 8a and b illustrate the above procedure. Here the mirror symmetry of the curve above  $T_{gs}$  is subtracted from the curve below  $T_{gs}$  in Figure 8a. The resultant curve is given in Figure 8b.

The double logarithmic plots of the data are presented in Figures 9 and 10 for the C2K4, C2Ca1 and C2Na8 samples. The critical exponents,  $\gamma$  and  $\beta$  were produced by fitting the data to the double logarithmic form of Eqs. (7) and (8) and are listed in Table 2, where it is seen that the average  $\beta$ (0.97) value is very close to the value of classical Flory – Stockmayer model.

However the observed average  $\gamma$ (0.71) is found to be little less than it is predicted in classical model. This discrepancy most probably originates from the shortcomings of

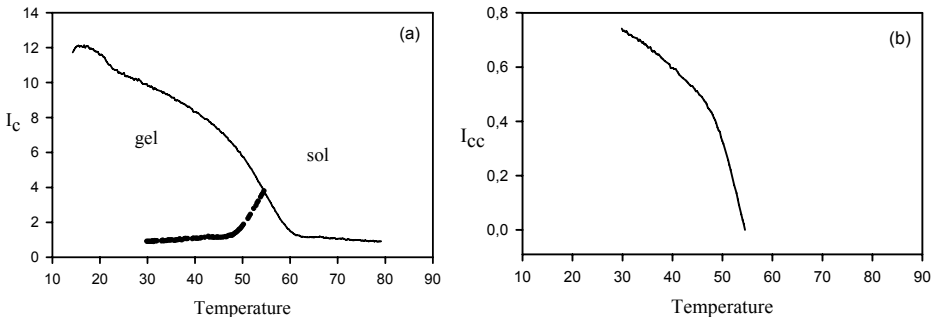


**Figure 8.** a) Subtraction of the mirror symmetry of  $I_c$  above  $T_{gs}$  from the curve below  $T_{gs}$ . b) The resultant  $I_{cc}$  curve present the pyranines embedded solely in the growing gel fraction,  $G$ .



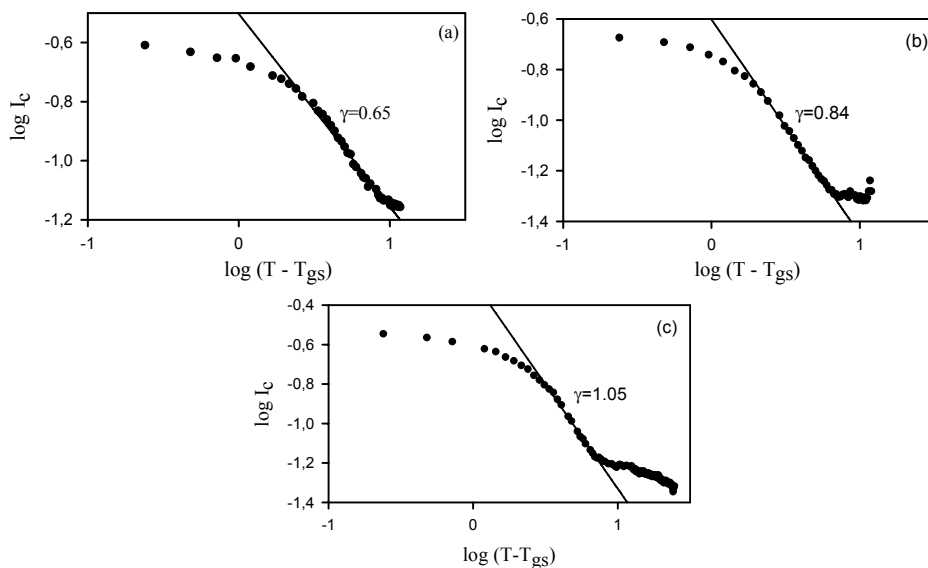


**Figure 9.** log – log plots of the data and their fits to Eq. 7 for a) C2K4, b) C2Ca1, c) C2Na8.

the fluorescence method in a give region. From here one may conclude that  $I_c$  measures the average coil (small cluster) size below  $T_{gs}$  during gel – sol transition paths. Whereas  $I_{cc}$  detects helices and double helices (gel fraction) during gel – sol transition paths above  $T_{gs}$ . Since the formation of gel from the helices and double helices should obey the classical Bethe lattice, the connection of helices and double helices must be in the Cayley tree form as seen in Figure 4.

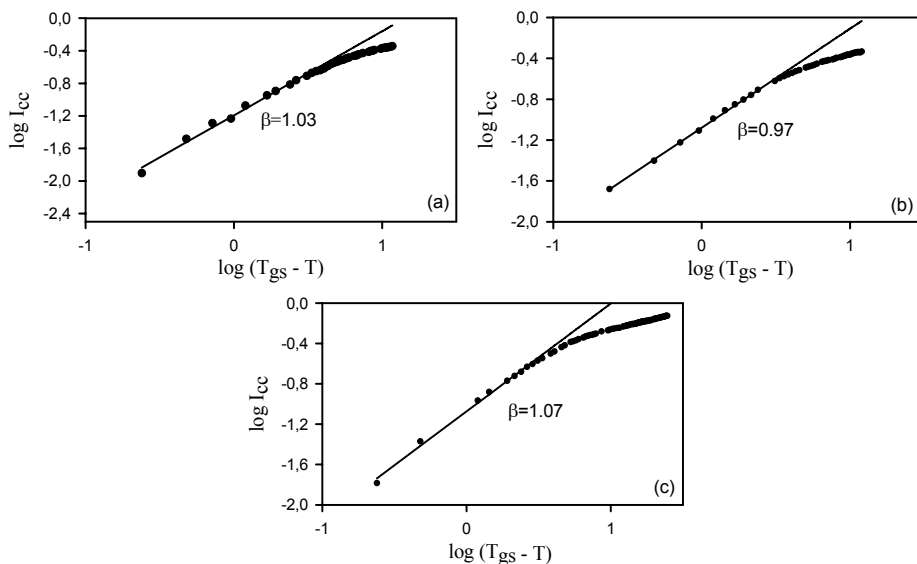


**Figure 10.** log – log plots of the data and their fits to Eq. 8 for a) C2K4, b) C2Ca1, c) C2Na8.

**Table 2.** The critical exponents  $\beta$  and  $\gamma$  for the gels in various  $KCl$ ,  $CaCl_2$  and  $NaCl$  solutions.

%KCl			%CaCl <sub>2</sub>			%NaCl		
Gels	$\beta$	$\gamma$	Gels	$\beta$	$\gamma$	Gels	$\beta$	$\gamma$
C2K0	0.95	0.55	C2Ca0	0.95	0.55	C2Na0	0.95	0.55
C2K2	0.93	0.54	C2Ca4	0.99	0.74	C2Na4	0.95	0.79
C2K4	1.03	0.65	C2Ca8	0.99	0.80	C2Na6	0.98	0.82
C2K8	0.93	0.20	C2Ca1	0.97	0.84	C2Na8	1.07	1.05
						C2Na1	0.95	0.88

## Conclusion

In conclusion, this paper has shown that the measured weight average degree of polymerization exponents,  $\gamma$  and gel fraction exponents,  $\beta$  obeyed classical Flory – Stockmayer model during the gel - sol transition. It is important to note that all carrageenan systems, independent of salt solutions are found to belong to the same universality class. In fact these results are consistent with our recent studies on acrylamide- carrageenan mixtures at high carrageenan concentrations, where  $\beta$  exponents obeyed classical Flory-Stockmayer model [31].

## References

- Papon P, Leblond J, Meijer PHE (2002) in: The Physics of Phase Transitions, translated from the French by S. L. Schnur, pp. 185-209. Springer, New York
- MacArtain P, Jacquier JC, Dawson KA (2003) Carbohydr Polym 53:395
- L. Piculell (1995) in: Food polysaccharides and their applications, A.M. Stephen (Ed.), pp. 205-244. Marcel Dekker, New York
- Viebke C, Piculell L, Nilsson S (1994) Macromolecules 27:4160
- Rochas C, Rinaudo M (1980) Biopolymers 19:1675
- Rochas C, Rinaudo M (1984) Biopolymers 23:735
- Morris ER, Rees DA, Robinson G (1980) J Mol Biol 138:349
- Hermansson AM, Eriksson E, Jordansson E (1991) Carbohydr Polym 16:297
- Watase M, Nishinari K (1982) Rheol Acta 21:318
- Watase M, Nishinari K (1988) J of Texture Studies 19:259
- Lai VMF, Wong PAL, Lii CY (2000) J Food Science 65:1332
- Michel AS, Mestdagh MM, Axelos MAV (1997) Int J Biol Macromol 21:195
- Hermanson A (1989) Carbohydr Polym 10:163
- Piculell L, Borgstrom J, Chronakis IS, Quist PO, Viebke C (1997) Int J Biol Macromol 21:141
- Watase M, Nishinari K (1985) Colloid Polym Sci 263:744
- Hugerth A, Nilsson S, Sundelöf LO (1999) Int J Biol Macromol 26:69
- Pekcan Ö, Yılmaz Y, Okay O (1997) Polymer 38:1693
- Pekcan Ö, Yılmaz Y, Okay O (1994) Chem Phys Lett 229:537
- Serrano B, Levenfeld B, Bravo J, Baselga J (1996) Polym Eng And Sci 36(2):175
- Yılmaz Y, Pekcan Ö (1998) Polymer 39:5351
- Güney O, Yılmaz Y, Pekcan Ö (2002) Sensors and Actuators B85:86
- Oya T, Enoki T, Yu Grosberg A, Masamune S, Sakiyama T, Takeoka Y, Tamaka K, Wang C, Yılmaz Y, Feld MS, Rasari R, Tanaka T (1999) Science 286:1543
- Pekcan Ö, Erdoğan M (2000) Polym Int 49:1641
- Stauffer D, Aharony A (1994) Introduction to Percolation Theory. Taylor and Francis, London

25. Sahimi M (1994) *Application of Percolation Theory*. Taylor and Francis, London
26. Flory PJ (1941) *J Am Chem Soc* 63:3083; 63:3091; 63:3096
27. Stockmayer WH (1943) *J Chem Phys* 11:45
28. Birks JB (1965) *Photophysics of aromatic molecules*. Wiley, London
29. Galanin MD (1995) *Luminescence of Molecules and Crystals*. International Science Publishing, Cambridge
30. Stauffer D, Coniglio A, Adam M (1982) *Adv Polym Science* 44:103
31. Aktaş DK, Evingur GA, Pekcan Ö (2006) *J Biomolecular Structure and Dynamics* 24:83